

New York University

# Hydroacoustic Modeling

Recreating underwater ambience

Mahin Salman and Hsin Hwa Tai

Advanced Musical Acoustics

August 13<sup>th</sup>, 2015

## **Introduction**

The theory of hydroacoustics has been contributed to by a number of physicists and mathematicians from Galileo, Newton and Leonardo da Vinci. The study of sound propagation underwater was perhaps most influenced by Lord Rayleigh's 'Theory of Sound', published in 1877. The onset of the First World War provided an impetus for further investigation and advancement in underwater acoustics. The study of sound underwater has been overlooked in the realm of Music Technology, largely due to the difficulty of obtaining high quality, underwater recordings. The purpose of this study is to conduct a controlled acoustics experiment that models ocean and freshwater environments using the principles studied over the duration of this course. The experiment should result in an impulse response that is of fair quality that can be used as an underwater reverb effect for composers.

## **Literature Review**

The majority of existing literature is focused primarily on ocean acoustics and modeling, nevertheless the same principles can be assumed for freshwater with adjustments to salinity and pH values. Acoustic energy is continually absorbed when sound propagates in the ocean. Additionally, sound scattering is affected by various inhomogeneities, which in turn decay sound intensity with range. Thus it becomes impossible to distinguish between absorption and scattering effects when conducting oceanic experiments (Brekhovskikh, 2003).

Sound absorption and scattering both contribute to sound attenuation underwater and behave similarly to sound in air but at a much faster speed. The literature infers that sound absorption in water is highly dependent upon temperature, salinity, depth and pH value. Acoustic absorption is significant for long-range propagation, particularly at higher frequencies, which attenuate much faster underwater than in air. As illustrated in Figure A. below.

While seafloor sediments are not being modeled for this study, it is significant to consider the impact they have on sound propagation and reflection. The structure of the ocean bottom becomes important when sound reaches the seafloor. Seafloor sediments are often modeled as fluids, which indicates that it will only propagate compressional waves. In reality, ocean beds are often viscoelastic and thus are also lossy.

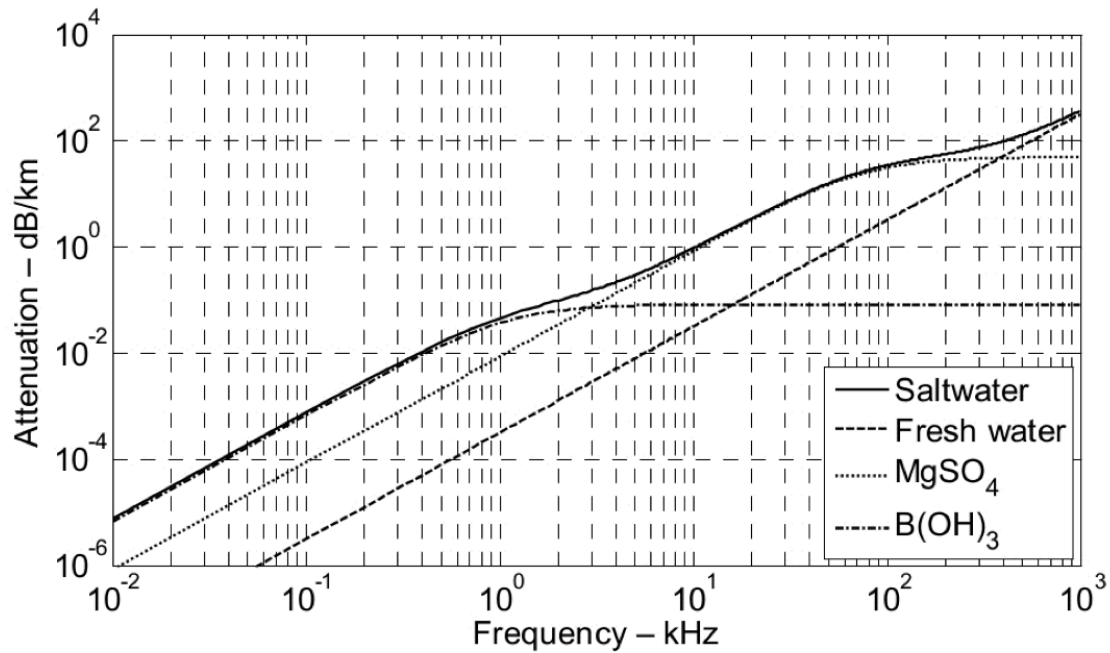


Figure A. Sound absorption as a function of frequency (kHz) for freshwater and saltwater at temperatures of 10C and atmospheric pressure of a single atmosphere (Hovem, 2013.)

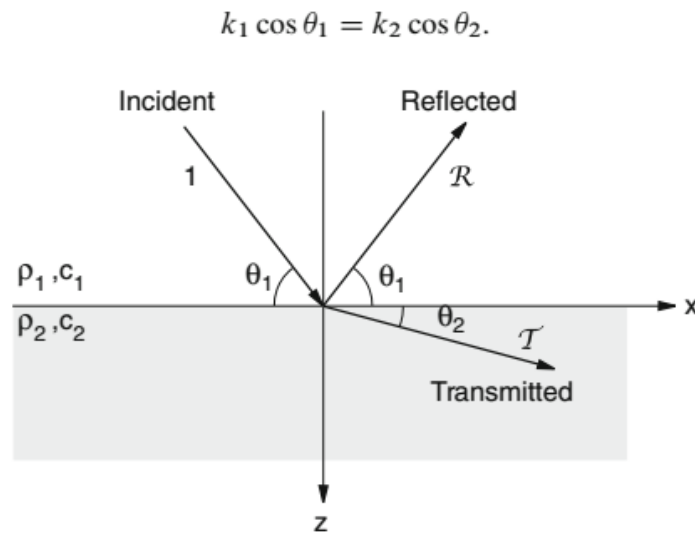


Figure B. Reflection and transmission from one fluid to another yields Snell's Law of Reflection (Brekhovskikh, 2003).

It is inferred that sound velocity is not continuous, and changes with depth. Furthermore, the salinity and temperature have an influence on the sound velocity. Depending on the stratification the temperature will also vary, thermal stratification is not unique to liquids and can also occur in air. In air, temperature changes can vary up to 10 °C within a meter range. However, in the thermocline most of the heat from the atmosphere is absorbed within the first few centimeters and then remains relatively stable. These changes in temperature in turn create zones with high or low sound pressure and thus there are often monotonous sound pressure changes with increasing distance from the sound source. Below the thermocline, the temperature remains constant at 2 °C but pressure increases thus increasing the speed of sound at this point despite the temperature drop (Muller and Zerbs, 2011).

As this study is based on experiments conducted in small tanks, it is imperative to consider velocity and absorption changes in shallow water. Shallow water can be categorized as a water depth below 200m and extremely shallow water is categorized at a water depth below 50m. Sound propagation in shallow water results in frequent reflections at the surface and increased refraction towards the ground. Propagation losses in this instance are determined by the properties of the ground. This makes the predictability of sound propagation in shallow water even more difficult than deep water (Muller and Zerbs, 2011).

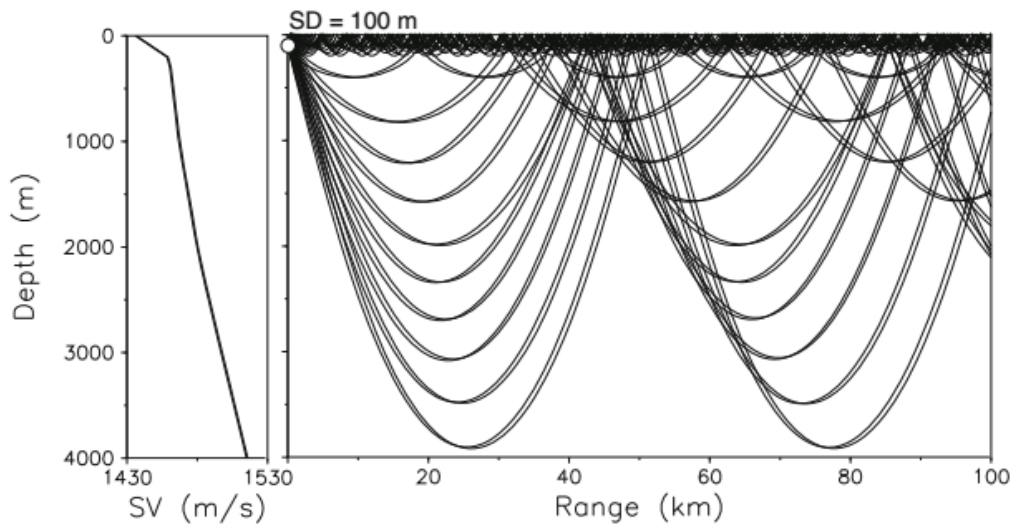


Figure C. Arctic propagation for 100 m deep source illustrating propagation paths and scattering loss with ice cover/sea ice at the surface. High frequency loss is a result of scattering from the rough underside of the ice. Low frequency loss is independent of this.

Sound propagation in the Arctic Ocean is characterized by even more complex reflections, salinity and temperature changes. With ice cover, an upward refracting profile is expected over the entire water depth, which causes energy to undergo recurring reflections particularly at the underside of the ice cover, as illustrated by Figure b. These reflections are further complicated by changes in temperature and lower surface salinity near the ice cover due to freshwater melting from the ice sheet. It is also imperative to note that low frequencies are not trapped by ice sheet cover but by seafloor sediments instead (Brekhovskikh, 2003).

## Methodology

The aim of the experiment is to find out how the speed of sound underwater alters sound characteristics. Furthermore, an impulse response will be obtained that will be convolved with audio stems. This will allow us to hear what it would actually sound like if we were within a contained underwater environment.

For the purpose of the experiment, the environment will be restrained within a static system. Whereas in a field study of an underwater acoustic environments, there would be multiple factors and complicated variables that influence sound propagation. The result will only altered by the variables being operated. There are four variables, tank size, temperature, salinity and ice cover. Additionally, since the recording devices have to be covered with waterproof protection, a calibration test will be performed to assess the impact of the waterproof protection.

Steps to be taken:

1. Calibration: A linear sine sweep is first recorded with the speaker and microphone, without being covered with waterproof protection. Then another recording is performed with the waterproof protection.
2. Measurement: In order to calculate the changes caused by each variable, measurements are required. This corresponds to the controlled variables of each experiment condition, the measurements include size of the tank (cm), depth of water(cm), temperature of water(Celsius), and amount of salt(g) which contributes to salinity levels.
3. Sound reproduction: For the purpose of reproducing sound underwater, the speaker needs to be wireless. The speaker will be connected via blue-tooth to playback a sine sweep from an iPhone. There are 2 types of sine tone generator that will be used to reproduce sine sweep in the experiment. The *F generator*, an iPhone tone generator app, reproduced 20.4 sec sine sweep from 20Hz to 20000Hz, and another pre-recorded 20 seconds and 40 seconds sine sweep from NCH Sound Tone Generator.

4. Five experiment conditions:
  1. Tub: Fresh water in large tub, normal room temperature(25 °C)
  2. Box 1: As 0 reference (Fresh water at 25 °C)
  3. Box 2: Temperature changed by adding ice (Fresh water at 4 °C, with ice floating on surface)
  4. Box 3: Temperature changed by adding ice (Fresh water at 4 °C, without ice floating on surface)
  5. Box 4: Salinity changed by adding salt (Saltwater with salinity at 3.4% )
5. Deconvolution of the impulse response: Once the recordings are obtained they will be processed through a deconvolve function coded in Matlab, which will result in the impulse response of the tank. The impulse response will then be convolved with audio stems to replicate how we would perceive sound underwater.

## **Apparatus**

- Shure SM57
- Audio interface for Mac: Echo Audiofire4
- Mac Book Pro with Pro tools 10
- Waterproof protection: Condoms, balloons, airtight diving bags
- Wireless speaker: Photive PH-BT1000
- Tonegenerator

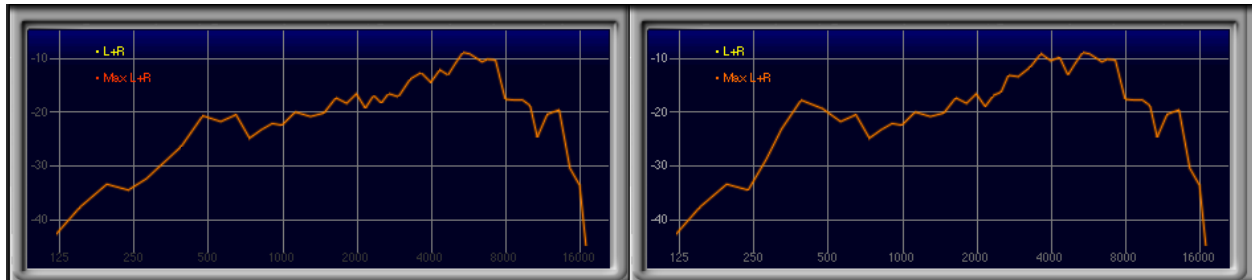
## **Hypothesis and Calculations**

Given the basic principle of underwater acoustics, the main differences between sound in air and underwater is the speed at which it propagates. The prediction can be discussed in two parts; the time domain and spectrum domain. In the time domain, the speed of sound underwater is approximately 5 times faster than in the air. The sound reflections are expected to overlap and sound blurred. As the experiments are being conducted in a static underwater environment, the principles of resonance are not expected to be influenced by a change in speed.

As the equipment will be waterproofed with various types of membranes, errors will be taken into account. Muffling of the sine sweep and the received signal will also be accounted for. Thus, it is anticipated that the results may not match our calculations entirely.

It is predicted that the SM57's will return the clearest results because they are a dynamic pair and closest to human hearing. Finally, the convolved audio will be

successful at imitating the underwater environment and can be used as an underwater reverb effect.



Graph 1: The spectrum analysis without (left)/ with(right) waterproofing.

### Tank Size:

Tub: 150 x 55 x 41(H) (cm)

Box: 39(L) x 27(W) x 21(H) (cm)

Other Measurement from recording:

Tub: Temp 25 °C/ Water depth 33 cm

Box1: Temp 25 °C/ Water depth 20.5 cm

Box2: Temp 4 °C/ Water depth 20.5 cm/ ice floating on surface

Box3: Temp 4 °C/ Water depth 20.5 cm/ ice water only

Box4: Temp 25 °C/ Salinity 3.4%/ Water depth 20.5 cm

### Equations for speed of sound underwater:

$c = 1449.2 + 4.6T - 0.055TT + 0.00029TTT + (1.34 - 0.01T)(S-35) + 0.016z$   
(Brekhovskikh, 2003).

T in centigrade

S part in thousand (% g/L)

z depth in meter

1. Tub:  

$$1449.2 + 4.6 \cdot 25 - 0.055(25)^2 + 0.00029(25)^3 + (1.34 - 0.01 \cdot 25)(0-35) + 0.016 \cdot 33$$

$$= 1449.2 + 115 - 34.375 + 4.53125 - 38.15 + 0.528$$

$$= 1496.73425$$
2. Box1(Fresh Water)  

$$1449.2 + 4.6 \cdot 25 - 0.055(25)^2 + 0.00029(25)^3 + (1.34 - 0.01 \cdot 25)(0-35) + 0.016 \cdot 20.5$$

$$= 1449.2 + 115 - 34.375 + 4.53125 - 38.15 + 0.328$$

$$= 1496.53425$$
3. Box2/3 (Ice water)  

$$1449.2 + 4.6 \cdot 4 - 0.055(4)^2 + 0.00029(4)^3 + (1.34 - 0.01 \cdot 4)(0-35) + 0.016 \cdot 20.5$$

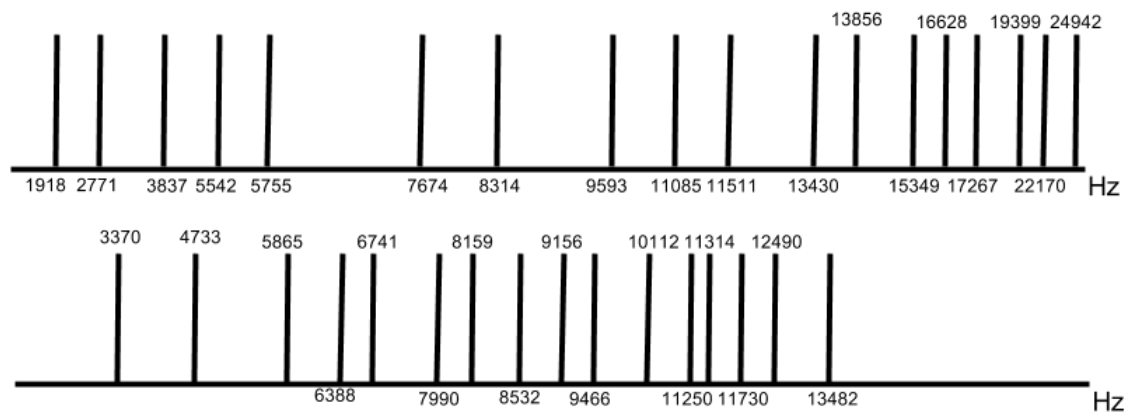
$$= 1449.2 + 18.4 - 0.88 + 0.01856 - 45.5 + 0.328$$

$$= 1421.56656$$

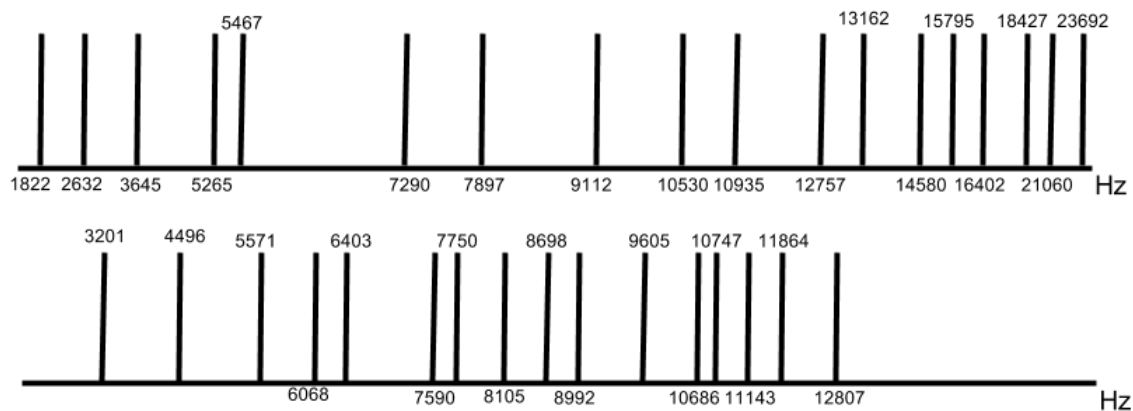
4. Box4 (all salt)  $S = 737g / 39 \times 27 \times 20.5 = 0.03414170893 = 3.4\%$   
 $1449.2 + 4.6 \times 25 - 0.055(25)^2 + 0.00029(25)^3 + (1.34 - 0.01 \times 25)(3.4 - 35) + 0.016 \times 20.5$   
 $= 1449.2 + 115 - 34.375 + 4.53125 - 34.444 + 0.328$   
 $= 1500.24025$

### Room Mode:

The room mode can be calculated (see index1) given by the speed of sound calculated above. It seems that the speed of sound is greatest in salt water, then fresh water, and slowest in cold water. Also, the differences among these three conditions are the density and temperature but not the size of the tank. The calculations of the room mode are identical to each other, which is also what is expected in the results.

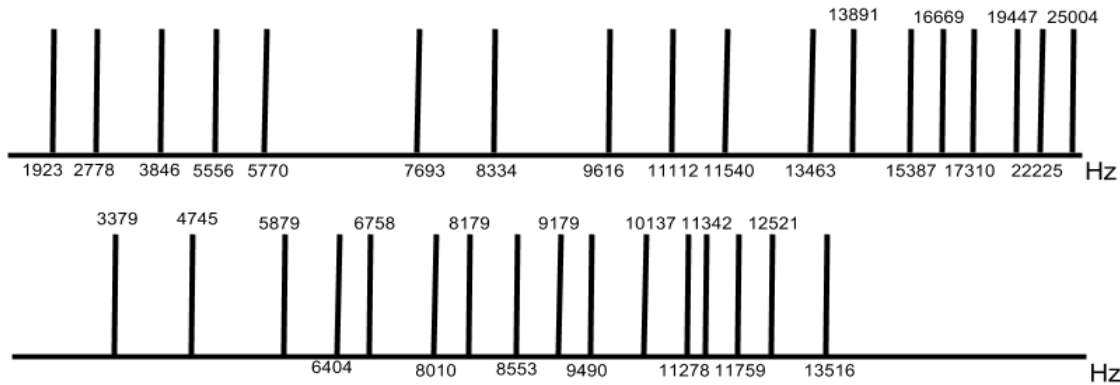


Graph 2-1. Axial and Tangential mode of fresh water



Graph 2-2. Axial and Tangential mode of cold water- slowest in speed which has the earliest room mode

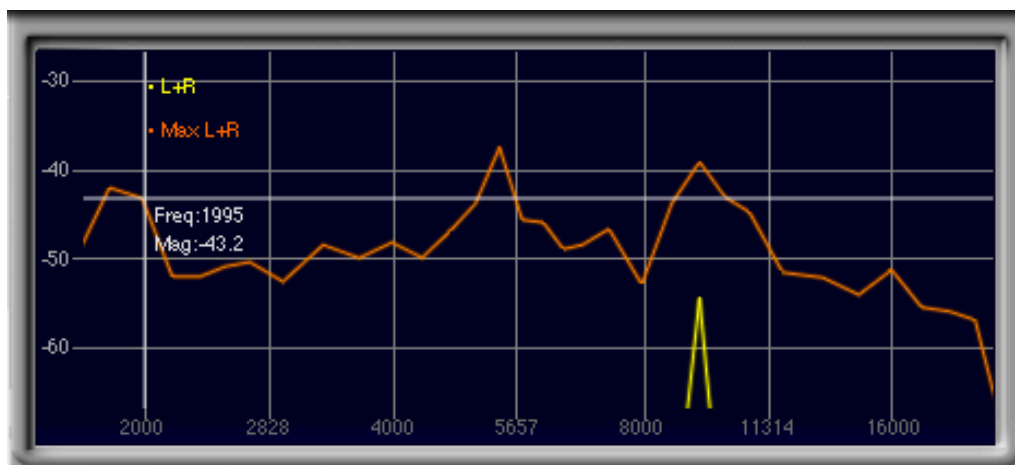




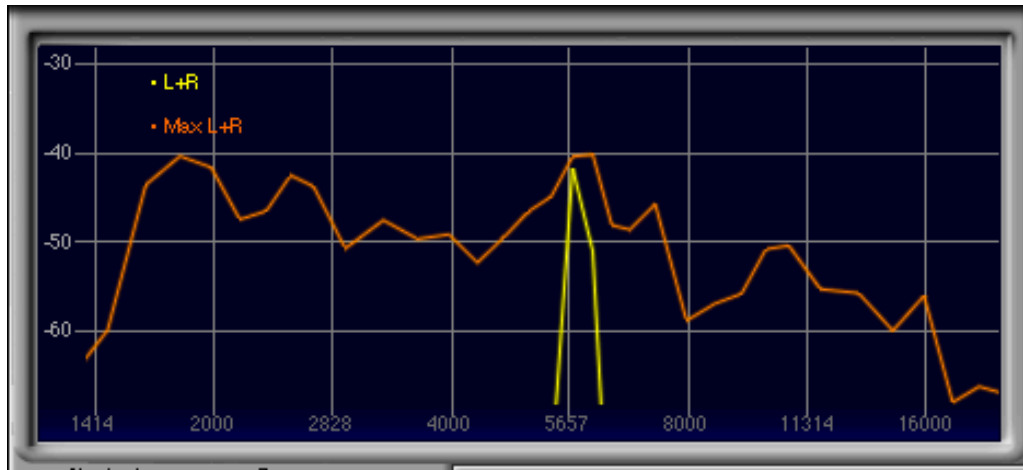
Graph 2-3. Axial and Tangential mode in salt water- greatest in speed which the room mode shows latest.

## Results and Discussion

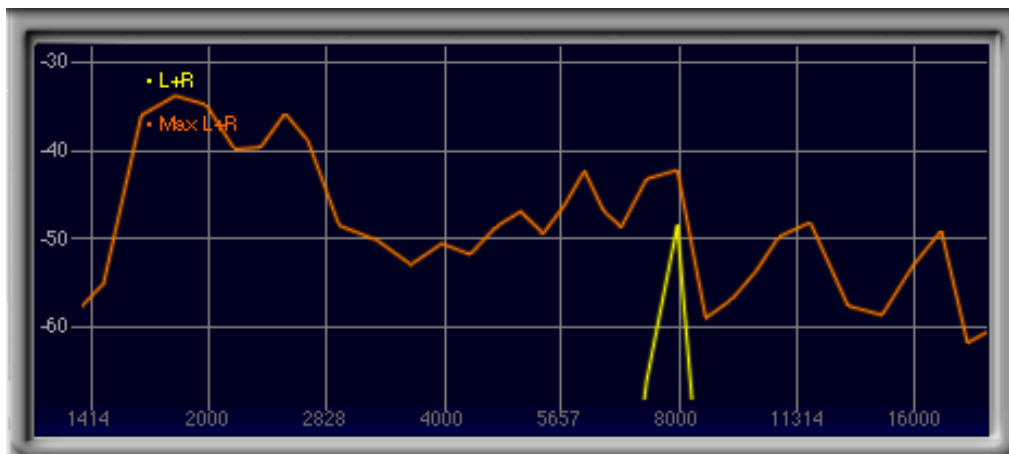
Given the sine sweep recording and spectrum analyzer, we can compare the differences between room mode calculation and the frequency response of the actual recording (graph 3-1, 3-2, and 3-3). The spectrum patterns, among the 3 measurements, are identical because the tank size is the same. Although the observed room mode doesn't precisely correspond to the calculated modes, we observed other predictions. First, the earliest room mode appeared to be cold water. Second, there are dips around 5kHz and 8kHz, which correspond to the axial mode. Finally, the interval of peaks is similar to the calculation. The axial mode shows at every 900Hz before 4kHz, which is also being seen in the measurement.



Graph 3-1 Fresh water



Graph 3-2 Ice water



Graph 3-3 Salt water

The recordings of the sine sweeps underwater were deconvolved using a Matlab function created for this study. As predicted our impulse responses contained continuous reflections which blurred the IR file. The audio contains a lot of noise which corresponds to the calibration test of the SM57 microphones. As noted earlier the, high frequencies decay earlier with waterproofing than without and the low frequencies were distorted by the vibrations of the waterproofing. These variations affected the impulse response file which sounds extremely noisy during playback. A further observation made during the experiments was that the lower frequencies created water waves in the tub and disturbed the stillness of the water in the smaller box. As a result, the movement of the water can be heard in the recorded sine sweeps, which also increased the noise factor in the impulse response files.

Furthermore, the increased reflectivity from the ice, increased salinity and shallowness of our test environment, contributed to distortions in our recordings. This agrees with our predictions as well as our literature, that sound propagation in shallow water is difficult to predict but also results in rapid and continuous reflections (Muller and Zerbs, 2011).

Essentially what happened during the deconvolution process is that the impulse response could not be effectively extracted/divided out of the recorded file because of the added distortions. Filtering the audio stems in Matlab did not return a successful result and due to shortage of time a specially designed filter could not be implemented.

The convolution of audio stems with the impulse response file returned excellent results. While the distortions did attenuate high frequencies, the overall affect of the underwater ambience is successful.

## Future work and Conclusion

It would be beneficial to conduct further experiments with increased modifications. As noted in the literature and discussion, ideally the experiments should be repeated in a larger tank and the reflections recorded with hydrophones. The larger tank would allow time for the higher frequencies to attenuate before reflecting and it may be possible to attain more accurate results on the room modes and decay curves. Furthermore, using hydrophones would surely return a higher quality recording as the waterproofed SM57 showed inconsistencies during calibration. Finally, it would be ideal to implement a filter design to reduce noise in the impulse response file, post deconvolution.

## Bibliography

- [1] F.B. Jensen et al., *Computational Ocean Acoustics*. Ch1 Fundamental of Ocean Acoustic. Modern Acoustics and Signal Processing, SpringerScience+BusinessMedia, LLC2011.
- [2] W.W.L. Au, M.C. Hastings, *Principles of Marine Bioacoustics*. Ch2 Measurement and Generation of Underwater Sounds. Pringer Science+Business Media, LLC 2008
- [3] Jens M. Hovem., "Ray Trace Modeling of Underwater Sound Propagation." 2013 Hovem
- [4] "Element of Ocean Engineering, CH8 Underwater Acoustic."
- [5] R.E. Francois, G.R. Garrison, Sound absorption based on ocean measurements. Part II: Boric acid contribution and equation for total absorption. J. Acoust. Soc. Am. 72, 1879–1890 (1982)
- [6] F.B. Jensen, W.A. Kuperman, Optimum frequency of propagation in shallow water environments. J. Acoust. Soc. Am. 73, 813–819 (1983)
- [7] A.Muller and C. Zerb, 'Measuring instructionsfor underwatersound monitoring' 2011

Integer s	Fresh Water 1496.53 m/s Mode Frequency (Hz)	Cold water 1421.57 m/s Mode Frequency (Hz)	Salt 1500.24 m/s Mode Frequency (Hz)	Axial	Tan gent ial
100	1918.63	1822.52	1923.38	X	
200	3837.27	3645.04	3846.77	X	
300	5755.90	5467.56	5770.15	X	
400	7674.53	7290.08	7693.54	X	
500	9593.17	9112.60	9616.92	X	
600	11511.80	10935.13	11540.31	X	
700	13430.44	12757.65	13463.69	X	
800	15349.07	14580.20	15387.80	X	
900	17267.70	16402.70	17310.46	X	
010	2771.36	2632.53	2778.22	X	
020	5542.72	5265.06	5556.45	X	
030	8314.08	7897.59	8334.67	X	
040	11085.44	10530.12	11112.89	X	
050	13856.80	13162.65	13891.11	X	
060	16628.16	15795.18	16669.34	X	
070	19399.51806	18427.71	19447.56	X	
080	22170.88	21060.25	22225.78	X	
090	24942.24	23692.78	25004.00	X	
110	3370.70	3201.84	3379.04		X
120	5865.40	5571.58	5879.92		X
130	8532.59	8105.16	8553.72		X
140	11250.25	10686.68	11278.11		X
210	4733.40	4496.28	4745.12		X
220	6741.40	6403.69	6758.09		X
230	9156.88	8698.18	9179.56		X
240	11730.80	11143.15	11759.85		X
310	6388.34	6068.317	6404.16		X
320	7990.75	7590.46	8010.54		X
330	10112.09	9605.53	10137.13		X
340	12490.69058	11864.98	12521.62		X
410	8159.60	7750.84	8179.80		X
420	9466.80	8992.56	9490.24		X
430	11314.70	10747.90	11342.71		X
440	13482.80	12807.37	13516.17		X

## Appendix

